Characteristics and formation of natural fractures in a silica-rich chalk, Coniacian Arnager Limestone Formation, Bornholm, Denmark

ASLAUG CLEMMENSEN GLAD, TOBIAS ORLANDER, IDA LYKKE FABRICIUS, OLE RØNØ CLAUSEN & LARS B. CLEMMENSEN

Geological Society of Denmark
https://2dgf.dk

Received 14 November 2023
Accepted in revised form
23 August 2024
Published online
18 October 2024

Glad, A.C., Orlander, T., Fabricius, I.L., Clausen, O.R. & Clemmensen, L.B. 2024. Characteristics and formation of natural fractures in a silica-rich chalk, Coniacian Arnager Limestone Formation, Bornholm, Denmark. Bulletin of the Geological Society of Denmark, Vol. 73, pp. 157–173. ISSN 2245-7070. https://doi.org/10.37570/bgsd-2024-73-09

Natural fractures are abundant and important components in many carbonate sedimentary rocks globally. In hydrocarbon and groundwater reservoirs of carbonate rocks they can form connected networks and thereby influence the permeability and fluid flow significantly. Outcrop studies of fractured carbonate rocks can provide an essential understanding of 3-dimensional fracture networks, thereby aiding in understanding fracture patterns and connectivity in subsurface carbonate reservoirs. The Arnager Limestone Formation is a naturally fractured silica-rich chalk of Coniacian age exposed in a coastal cliff on the island of Bornholm in the Baltic Sea (Denmark). This study examines the natural fractures in the Arnager Limestone Formation from a structural and geomechanical perspective. The Arnager Limestone Formation forms one, 12–20 m thick, main rock mechanical unit; bedding planes acts as weak interfaces and divides it into near-identical, cm- to dm-thick rock mechanical subuits. Flat-lying (horizontal) or low-angle dipping bedding-parallel fractures are intersected by two near-vertical or steeply dipping fracture systems, a major N–S-trending system and a less prominent W–E-trending fracture system. Rock mechanical analysis of the tensile strength and elastic moduli provides the foundation for discussing maximum burial depth of the Arnager Limestone Formation. The tensile strength gives information on the bedding-parallel fractures, which can have formed due to stress relief during uplift and erosion, possible accentuated by glacial processes. The near-vertical fracture sets are interpreted to have formed in response to tectonic movements.

Keywords: Arnager Limestone Formation, silica-rich chalk, natural fractures, rock mechanical properties, Bornholm.

Aslaug Clemmensen Glad [Aslaug.Clemmensen.Glad@Bluenord.com], Bluenord, Lyngbyvej 2, 2100 Copenhagen, Denmark and The Danish Offshore Technology Centre, Technical University of Denmark, Elektrovej 375, 2800, Kgs. Lyngby, Denmark. Tobias Orlander [TOR@geo.dk], The Danish Offshore Technology Centre, Technical University of Denmark, Elektrovej 375, 2800, Kgs. Lyngby, Denmark; present address: Geo – Subsurface Expertise, Maglebjergvej 1, 2800 Kgs. Lyngby. Ida Lykke Fabricius [ilfa@dtu.dk], DTU Department of Environmental and Resource Engineering, Technical University of Denmark, Brovej 118, 2800, Kgs. Lyngby, Denmark. Ole Rønø Clausen [ole.r.clausen@geo.au.dk], Department of Geoscience, Aarhus University, Høegh-Guldbergs Gade 2, 8000 Aarhus. Lars B. Clemmensen [larsc@ign.ku.dk], Department of Geosciences and Natural Resource Management, University of Copenhagen, Øster Voldgade 10, 1350 Copenhagen, Denmark.

A natural fracture forms in response to stress as a mechanical breakage or discontinuity (Wolfsberg 1997; Gudmundsson 2011). Fractures are ubiquitous and prominent constituents of carbonate sedimentary rocks both in the subsurface and in outcrops. They can have a significant influence on the host rock by enhancing the local permeability by orders of magnitude, forming connected pathways for fluid flow, alter the rock strength and impact the petrophysical properties of the rock (Gabrielsen & Koestler 1987; Aguilera 1998; Bratton *et al.* 2006; Lemonnier & Bourbiaux 2010; Ogata *et al.* 2014). Interpretation of fracture patterns, interactions and crosscutting relationships can function as indicator for palaeostress and thereby earlier tectonic episodes (Price & Cosgrove 1990).

Extensive deposition of chalk occurred during the Late Cretaceous across Northwestern Europe with the youngest sediments of Maastrichtian and Danian (Palaeogene) age constituting important reservoirs for both hydrocarbons in the North Sea and groundwater in Denmark, Germany, France, Belgium, the Netherlands, and Britain. Scarce data, based on wells situated kilometers apart, often constrain subsurface understanding of fracture systems, and thus to optimise the understanding of fracture systems in chalk, outcrop studies can provide important insights into the geometry of fractures, their internal relationship, and lithological control on fracture formation.

The Coniacian Arnager Limestone Formation (hereafter Arnager Limestone) is exposed in a coastal cliff at the south coast of Bornholm (Fig. 1). The Arnager Limestone, which is a silica-rich chalk, possesses a well-developed fracture network briefly mentioned by e.g. Hart *et al.* (2012) and Svennevig & Surlyk (2018). However, so far, no detailed characterisation and interpretation of this fracture network have been given. The limestone contains flat-lying (horizontal) to low-angle dipping bedding-parallel fractures intersected by near-vertical to steeply dipping fractures resulting in a block-like appearance of the limestone (Fig. 2).

The purpose of this study is to describe and interpret the origin of the natural fractures in the Arnager Limestone. Bedding-parallel fractures are linked to petrophysical and mechanical properties of the limestone, including porosity, elastic wave velocities, elastic moduli, and tensile strength, and a new estimate of palaeoburial depth of the Arnager Limestone is proposed. Fracture orientation of the near-vertical to steeply dipping fractures are described and their origin discussed in relation to the tectonic evolution of the area.

Geological setting

Structural framework

The island of Bornholm (55°N, 15°E), forms a horst block and is part of the Sorgenfrei–Tornquist Zone that separates the Baltic Shield from the Danish and North German Basins (Graversen 2004, 2009; Fig. 1). Precambrian granites, migmatites and gneisses with ages of approximately 1.4 Ga (Waight *et al.* 2017) are exposed in the northern part whereas faulted Palaeozoic and Mesozoic sedimentary rocks outcrop in the

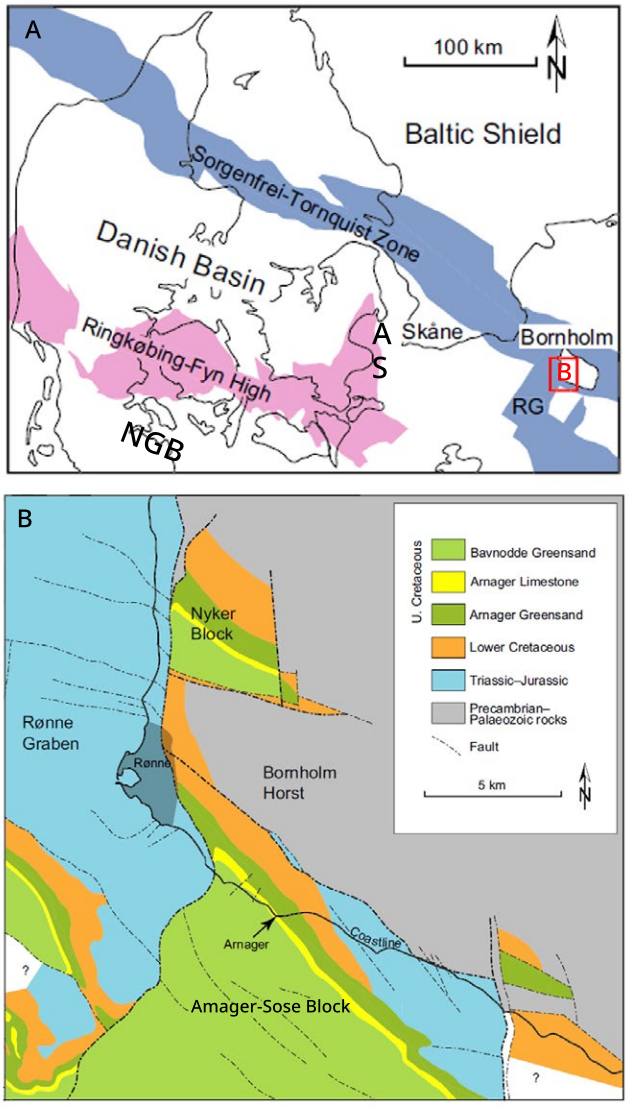

Fig. 1. A, Structural setting of Bornholm in the Sorgenfrei–Tornquist zone; NGB: North German Basin; RG: Rønne Graben; S: Stevns; A: Amager. **B,** Geological map of the south and west coast of Bornholm and nearby coastal areas. The Arnager Limestone Formation is exposed in a coastal cliff at Arnager on the south coast of Bornholm (maps after Svennevig & Surlyk 2018).

southern and south-eastern part. Bornholm is part of the Tornquist lineament at the transition between the Danish-Swedish Sorgenfrei–Tornquist Zone and its southwards continuation towards Poland (Michelsen & Nielsen 1991; Erlström *et al.* 1997; Cotte & Pedersen 2002; Babuska & Plomerova 2004; Lykke-Andersen & Surlyk 2004; Madsen *et al.* 2010). The sedimentary rock exposures are controlled by a series of northwest–southeast striking faults defining the trend of the Tornquist lineament; these major faults are linked by approximately north–south-trending faults running parallel to the Rønne Graben, which is located just offshore the west coast of Bornholm (Vejbæk 1985; Jensen & Hamann 1989).

Late Cretaceous deposits on Bornholm comprise the Arnager Greensand Formation (Cenomanian), the Arnager Limestone Formation (Coniacian), and the Bavnodde Greensand Formation (Coniacian–Santonian) with the Arnager Limestone being confined to the Arnager-Sose Block and a minor exposure on the Nyker Block towards the north. During the Late Cretaceous, Bornholm was situated at a palaeolatitude of 48°N in a boreal realm (Ziegler 1990).

The Mesozoic tectonic evolution of the Bornholm area was characterised by repeated block faulting (Graversen 2009). The geometry of the Mesozoic faults was analysed by Graversen (2009), and the cumulative directions of the faults indicate that most faults on the Mesozoic Arnager-Sose block trend NW–SE (315–135°) with only little variation; a few faults are aligned W–E (275–95°) and NNW–SSE (345–165°). According to Graversen (2009) the Mesozoic fault systems are

Fig. 2. The cliff exposure at Arnager. The Arnager Limestone Formation overlies the Arnager Greensand Formation (green-grey); a complex conglomerate (arrow) occurs at the boundary between the two units. There is a hiatus, but no angular unconformity between the two formations. Both formations have been tilted with identical low angles towards the NW. The Arnager Limestone (exposed thickness here 5–6 m) has a lower unit with mound bedding, and an upper, thinner unit with flat bedding; the bedding in the uppermost part of this unit has been disrupted due to glacial impact. The two formations define two different rock mechanical units. A fracture system composed of two near-vertical and orthogonal fracture sets and a flat-lying to low-angle dipping, bedding-parallel fracture set is seen in the Arnager Limestone Formation; fractures are absent in the Arnager Greensand Formation. Cliff is viewed from the southeast.

related to three-dimensional strain with maximum extension striking NE–SW and secondary extension striking NW–SE. Tectonic activity in the Late Cretaceous and Paleogene caused an inversion of the block and erosion of overlying sediments (Graversen 2004).

Bornholm was covered by the Scandinavian Ice Sheet several times during the Quaternary. In the Weichselian, the ice sheet may have reached a maximum thickness of about 1500 m (Humlum & Houmark-Nielsen 1994; Houmark-Nielsen 2011); the ice retreated 16,000 years ago resulting in the formation of proglacial meltwater deposits at many sites including the Arnager area. These repeated episodes of glacial advance and retreat may have impacted the deformation history of the Arnager Limestone.

Stratigraphy and sedimentology

The Arnager Limestone is of Late Cretaceous (Early to Middle Coniacian) age (Svennevig & Surlyk 2018), and well exposed in a coastal cliff on the south coast of Bornholm immediately to the northwest of the village of Arnager (Figs 1, 2). The Arnager Limestone has here a thickness of 12 to 20 m and overlies the Middle Cenomanian Arnager Greensand Formation (hereafter Arnager Greensand; Svennevig & Surlyk 2018). There is a complex conglomerate of glauconitised and phosphatised pebbles at the boundary between the Arnager Limestone and the underlying Arnager Greensand (Hart *et al.* 2012). The Arnager Limestone is overlain by the up to 180 m thick Late Coniacian to Early Santonian Bavnodde Greensand Formation (hereafter Bavnodde Greensand; Christensen 1985; Packer & Hart 2005; Svennevig & Surlyk 2018); the Bavnodde Greensand rests on the eroded surface of the Arnager Limestone (Packer & Hart 2005). In the studied coastal cliff section, the Arnager Limestone is unconformably overlain by Quaternary deposits.

The Arnager Limestone forms a hard, silica-rich chalk with a macrofauna dominated by siliceous sponges in association with relatively sparse inoceramid bivalves, other bivalves, brachiopods, belemnites and rare ammonites (Svennevig & Surlyk 2018). The chalk is strongly bioturbated with common trace fossils including *Thalassinoides*, *Condrites*, *Zoophycos*, *Planolites* and *Teichichnus* (Noe-Nygaard & Surlyk 1985; Svennevig & Surlyk 2018). No observations of stylolites have been reported.

The matrix of the limestone is composed of fine-grained opal-CT embedded in biogenic partly recrystallised carbonate material (coccoliths, crystallites of coccoliths and shell detritus), SEM images of the latter can be found in Madsen *et al.* (2010). The carbonate content of the sediment typically varies between 45 and 70% by weight (Tröger & Christensen 1991; Noe-Nygaard & Surlyk 1985). Cemented contacts between carbonate particles occur, but no porosity-reducing carbonate cement has been noted as can be seen in the SEM-images in Madsen *et al.* (2010). The silica is diagenetic and probably formed by precipitation of opal-CT sourced by siliceous sponge spicules, which are present as moulds (Madsen *et al.* 2010). The silica content varies between 30 and 50% (Madsen *et al.* 2010). Locally opal-CT has transformed into quartz (Madsen *et al.* 2010). The limestone contains some clay; between 0.4 and 5.4%, with typical values between 1 and 2% (Svennevig & Surlyk 2018).

The Arnager Limestone can be divided into two parts: 1) a lower part with a thickness of 4–5 m which is primarily composed of mound-bedded strata and 2) an upper part comprising the remaining part of the succession primarily composed of flat-bedded strata (Noe-Nygaard & Surlyk 1985); the uppermost part of the limestone has no or poor bedding due to impact by glacial processes. The mounds in the lower part are 6–8 m wide and 1–2 m high; their flanks dip 5–10° (Noe-Nygaard & Surlyk 1985). Individual beds vary between 5 and 30 cm in thickness and are commonly accentuated and dissected by fractures (see later).

In the mound-bedded part of the limestone two microfacies occur: spiculitic wackestone and bioturbated spiculitic wackestone. The former microfacies has porosity of 36–42% with an average of 39%, and permeability of 4–20 mD with an average of 12 mD (Madsen *et al.* 2010). The latter microfacies have porosity values between 12 and 41% with an average of 38%, and permeability of 5–13 mD with an average of 10 mD (Madsen *et al.* 2010). In this study, however, all limestone is treated as one uniform facies.

The complex conglomerate at the boundary between the Arnager Limestone and the Arnager Greensand (Fig. 3) was divided into a number of sedimentary units by Bromley (1979) and Hart *et al.* (2012). According to Hart *et al.* (2012) a lower unit overlies soft glauconitic sand and is composed of somewhat lithified glauconitic sandstone with phosphatised clasts. Hart *et al.* (2012) mentioned a thickness of about 1 m for this unit, however, recent exposures only show a thickness of around 0.3 m. This unit is penetrated by large *Thallassinoides* burrows and is overlain by a surface (hardground) marked by large glauconitised and/or phosphatised clasts (Bromley 1979). Above the hardground associated with large clasts lies a sandy limestone with scattered, relatively small glauconitized and/or phosphatised clasts. Hart *et al.* (2012) suggested that this upper unit has a thickness of around 0.5 m while current exposures are 0.1–0.2 m thick. According to Hart *et al.* (2012), the lower conglomerate unit belongs to the Arnager Greensand Formation, while the upper unit is part of the Arnager

Limestone Formation. Two samples from the boundary conglomerate have a porosity of respectively 29 and 38% and permeability of 1.3 and 1.7 mD (Madsen *et al*. 2010). However, it is unclear which part of the conglomerate these samples represent.

The underlying Arnager Greensand consists of an unconsolidated, poorly sorted, fine-grained quartz sand with abundant glauconite (Solymar & Fabricius 1999). The formation contains a few layers of cemented, coarse-grained sandstone. Laboratory investigation of samples from the uppermost part of this formation gives porosity values between 39 and 44% and permeability between 11 and 29 mD (Solymar & Fabricius 1999).

The overlying Bavnodde Greensand consists of unconsolidated, poorly sorted, glauconitic, fine-grained, silty quartz sand. The formation contains a number of cemented quartz sandstones (Christensen 1985).

In a mechanical stratigraphical framework, the Arnager Limestone is here considered to form one, 12–20 m thick, mechanical unit in agreement with the definition of Cooke *et al*. (2007). However, at a later stage during the Quaternary the uppermost part of the formation has been subjected to glacial forces resulting in disintegration of the bedding. Bedding planes within the limestone act as weak mechanical interfaces and thereby subdivide the limestone into a number almost identical, 0.06 to 0.4 m thick, mechanical subunits. A major mechanical interface is defined by the hardground in the middle of the boundary conglomerate that thereby separates two main rock mechanical units, i. e. the Arnager Greensand and the Arnager Limestone.

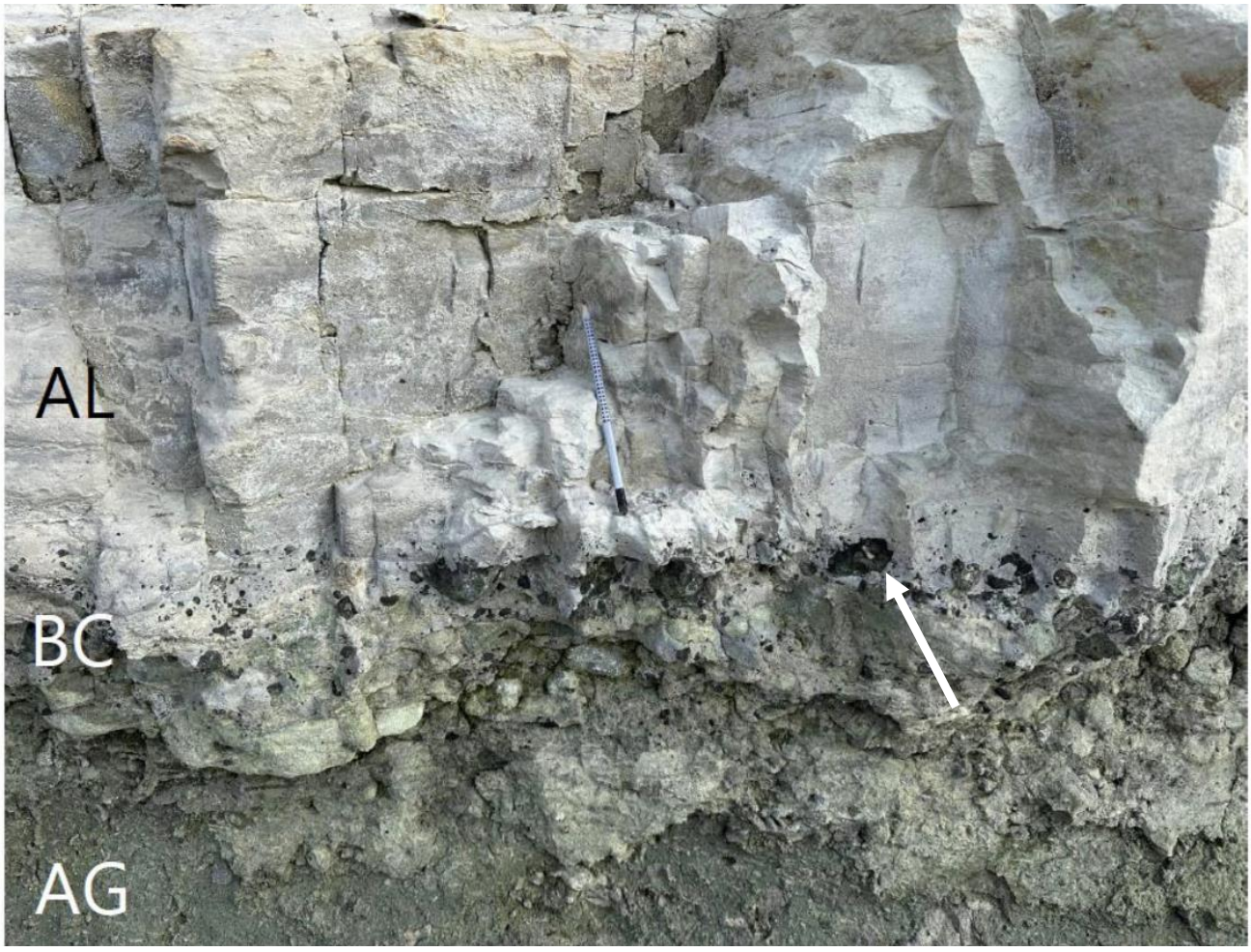

Fig. 3. The boundary conglomerate (BC) forms the transition zone between the Arnager Greensand Formation (AG) and the Arnager Limestone Formation (AL). The boundary conglomerate can be divided into a lower part (belonging to the Arnager Greensand Formation) formed by somewhat lithified glauconitic sandstone with phosphatised clasts and an upper part (belonging to the Arnager Limestone Formation) formed by sandy limestone with scattered, relatively small glauconitised and/or phosphatised clasts; there is a hardground associated with large, dark clasts at the boundary between the two units (arrow). Note that the near-vertical fractures in the Arnager Limestone Formation lose their identity in the upper part of the boundary conglomerate and are absent below the hardground. Pencil for scale.

Methods

Fracture description

The term fracture has been used to describe a range of structures, including faults, joints, veins, dykes, sills, deformation bands, and stylolites (Peacock *et al.* 2017). Fractures that occur within a specific formation/rock unit are termed a fracture system. When individual fractures have similar properties and a well-defined orientation, they can be termed a fracture set (Peacock *et al.* 2017). The spatial arrangement of various fracture sets forms a fracture network; fractures intersect at intersection points (nodes) or intersection lines (Peacock *et al.* 2017).

Six cliff sections in the lowermost mound-bedded part of the Arnager Limestone were selected for this study of fractures. Investigated sections were about 5 m in width and 2 m in height. Moving along the cliff towards the NW the investigated sites represent increasingly higher levels in the stratigraphy. All sites presented a well-developed fracture network in the mound-bedded part of the limestone. The sections were photographed, and fracture types were recorded. The blocky structures of the limestone made it possible to measure strike and dip of the near-vertical to steeply dipping fractures on exposed fracture surfaces. Supplementary investigation of these fractures was carried out on bedding plane exposures seen at low water level on the wave-eroded platform in the beach zone or at the foot of the cliff. On these bedding planes additional data on fracture orientation and spacing was obtained. Flat-lying or low-angle dipping fractures closely follow bedding contacts and are here named bedding-parallel fractures.

Data on spacing of both fracture types were collected along the entire cliff section. At all sampling sites, the spacing of bedding-parallel fractures (bed thickness) was measured in a vertical section of approximately 2 m, while spacing of sub-vertical to steeply dipping fractures was measured in one of the beds. No apparent variation was observed along the cliff exposure.

Rock mechanical testing

Blocks of silica-rich chalk were taken in the lower mound-bedded part of the Arnager Limestone along the cliff section. Samples were taken from different beds of identical visual appearance and considered to have near-identical mechanical properties due to similarity in induration. Around 75 cylindrical plug/disk samples were prepared from the block samples for tensile strength measurements of the vertical (V), horizontal north-west (HNW) and horizontal north-east (HNE) directions (Table 1). The tensile strength was measured using the Brazil test (ISRM 1978), a method suggested for determining the indirect tensile strength, where each disk was loaded between two curved plates until splitting.

The normal splitting load was recorded (P), and the indirect tensile strength (σ_T) calculated as

$$\sigma_T = \frac{2P}{\pi d l} \quad (1)$$

where d and l are the diameter and thickness/length of the disk, respectively.

Five vertical core plugs denoted as S1 to S5 with approximate dimensions of 37 mm diameter and 25 mm length (Table 1) were prepared for advanced testing and cleaned for salt using methanol as the solvent in soxhlet extraction (Dean 1998). Cleaned plug samples were oven-dried at 60˚C before being equilibrated to ambient temperature in a desiccator. Grain density was determined from gas porosimetry by N_2 expansion, and the dry density was derived from dry mass and plug dimensions. In the dry state and at uniaxial stress of 1.5 MPa, we transmitted and recorded one compressional wave (P) and two orthogonal shear waves (S1 and S2) in the longitudinal plug direction. The output frequency of the P- and S-waves is approximately 300 kHz and 600 kHz, respectively. Arrival times corrected for system delay were combined with deformation-corrected plug length to derive elastic P- and S-wave velocities (V_P and V_S).

The elasticity of a porous medium describes the resistance to elastic deformation (strain, ε) and is commonly described in terms of an elastic modulus. By combining the elastic wave velocities with dry density (ρ_{dry}), the dry dynamic compressional (M_{dry}) and shear (G_{dry}) modulus were derived as

$$M_{\mathrm{dry}} = \rho_{\mathrm{dry}} V_{\mathrm{P}}^2 \quad (2)$$

$$G_{\mathrm{dyn}} = \rho_{\mathrm{dry}} V_{\mathrm{S}}^2 \quad (3)$$

Poisson's ratio (ν) defines the ratio of transverse strain (ε_T) (perpendicular to the loading direction) to vertial strain (ε_V) and may be derived through a combination of (M_{dry}) and shear (G_{dry}) as

$$\nu = \frac{\varepsilon_T}{\varepsilon_V} = \frac{M_{dry} - 2G_{dry}}{2M_{dry} - 2G_{dry}} \quad (4)$$

Table 1. Properties of samples from the Arnager Limestone Formation.

ID	Diameter d mm	Length l mm	Dry mass m_{dry} g	Dry density ρ_{dry} g/cm^3	Grain density ρ_s g/cm^3	Porosity ϕ %	Elastic velocity V_p km/s	V_s km/s	Dry dynamic moduli and Poisson's ratio M_{dry} GPa	G_{dry} GPa	v -	Dry tensile strength σ_T[7] MPa
S1[1]	37.32	26.20	42.99	1.50	2.69	44.2[5]	2.26	1.53	7.65	3.54	0.07	
S2[1]	37.22	25.43	37.28	1.35	2.70	50.2[5]	1.84	1.25	4.58	2.10	0.07	
S3[1]	37.35	26.94	43.74	1.48	2.71	45.3[5]	1.72	1.13	4.36	1.89	0.12	
S4[1]	37.31	27.48	45.88	1.53	2.69	43.2[5]	2.23	1.47	7.62	3.28	0.12	
S5[1]	37.28	27.11	45.46	1.53	2.65	42.4[5]	2.22	1.44	7.50	3.19	0.13	
Average					2.69	45.1	2.05	1.37	6.34	2.80	0.10	
Stdandard deviation					0.02	3.1	0.26	0.17	1.71	0.75	0.03	
V1-V22[2]	35.73-37.90	16.16-22.27	26.29-40.85	1.32-1.67		37.9-50.7[6]						3.6-19.2
HNW1-HNW27[3]	37.04-37.91	15.18-21.75	25.25-38.61	1.34-1.72		35.9-50.2[6]						1.7-14.5
HNE1-HNE2[4]	37.55-38.08	15.53-22.68	24.71-38.32	1.34-1.66		38.2-50.1[6]						2.6-12.3 2.6-12.3
Average												8.2
Standard deviation												3.6

[1] Vertical samples used for advanced testing.
[2] Veritial samples used for tensile strength.
[3] Horizotal north-west samples used for tensile strength.
[4] Horizotal north-east samples used for tensile strength.
[5] N_2 porosity.
[6] Calculated from dry density and average grain density.
[7] Indirect dry tensile strength from Brazil testing.
M, *G* and *v* are compressional modulus, shear modulus and Poisson's ratio, respectively.

Results

Fractures

The coastal cliff is 200 m long, beginning just west of the harbour in the village of Arnager (Fig. 2). The cliff has a somewhat irregular appearance with an overall NW–SE-orientation. The Arnager Limestone has an apparent dip of 5° towards the NW (parallel to the cliff) resulting in the lowest stratigraphic levels being exposed towards the SE; from the central part of the cliff exposure and towards the SE, the boundary conglomerate and the uppermost part of the Arnager Greensand are exposed (Fig. 2).

The fracture system of the Arnager Limestone is composed of both bedding-parallel fractures and sub-vertical to steeply dipping fractures; these interacting fractures give the limestone in the cliff exposure a block-like appearance (Fig. 2). In the lower part of the cliff, these blocks have a typical width of 0.07–0.15 m and a typical height between 0.06 and 0.20 m. Towards the top of the cliff (and the Quaternary overburden), these block structures get smaller and smaller, frequently disintegrating into near rubble conditions. Thus, our measurements of fracture characteristics have been carried out in the lower 2 m of the exposed section where the fractures are best defined and easy to study.

At all the six sites studied, the limestone shows a well-defined bedding. All sites were characterised by more or less well-developed mound bedding with flanks that dip 5–10° (Noe-Nygaard & Surlyk 1985). Internally these banks show strata that dip in both directions. Bed boundaries are characterised by thin fractures (bedding-parallel fractures); these are flat-lying or show gentle dips in accordance with the architecture of the mound structure. Rarely, however, there were signs of lithological change along these fractures/bedding planes. In a few cases, mm-thin clay-rich material was observed at the top of a limestone bed supporting the interpretation that the top of this bed is a true bedding plane.

The bedding-parallel fractures, both those associated with the flat-bedded and the mound-bedded

strata, are intersected by two near-vertical to steeply dipping fracture sets; one set is trending N–S (355–175°) and a second set is trending W–E (265–85°; Fig. 4). Fracture orientation and spacing did not show any apparent change along the cliff or across the mound structure. In the middle part of the cliff section wave-eroded platforms with fractures were observed at the cliff foot.

The cliff exposures illustrate the broken-up structure of the limestone with the two orthogonal, steeply dipping fracture sets and the bedding-parallel fracture set (Figs 2, 5). The traces of the N–S fracture set on cliff sides are straight to somewhat undulatory and near vertical. Accordingly, exposed block surfaces controlled by these fractures possess dip angles around 85°. The block surfaces controlled by W–E-trending fractures have less steep dip angles; typically, they vary between 75° and 85°. The traces of these fractures in cliff exposures are straight to somewhat undulatory and have an appearance similar to the N–S-trending fractures.

Visual inspection of the selected sites shows that few N–S-trending fractures are restricted to one bed (mechanical subunit), while most are confined to 2–5 beds and more rarely up to 10 beds (Fig. 5). Many of the fractures show minor sidewards displacement when crossing a bed boundary (weak mechanical interface), and it may therefore be difficult to decide whether such a displaced fracture should be classified as a new fracture or as the original one. A limited number of fractures can be traced from bottom to near the top of the exposure and thereby span the complete mechanical unit of the Arnager Limestone (Fig. 6).

Bedding plane exposures were seen in two levels; one immediately above the boundary conglomerate and one around 1 m above this conglomerate (Fig. 7). On the very low-angle dipping bedding plane exposures, the two sub-vertical to steeply dipping fracture sets are viewed on relatively clean surfaces; it is apparent that one set is trending NNW–SSE and a second set is trending W–E. The two fracture sets are seen to be cross cutting in some places with no or minor offsets at intersection points.

Fracture width of the steeply dipping fractures (aperture) in cliff exposures is typically up to 1 cm; when undisturbed by recent disintegration, fracture width, however, is only a few millimetres. Observations on bedding planes also indicate that the width of these fractures is rarely more than a few millimetres. Fracture coatings or cement were not observed. Fracture width of the bedding-parallel fracture is also up to 1 cm.

Measurement of the spacing of the near-vertical to steeply dipping fractures was carried out at all six sites and confined at each site to one bed. N–S-trending fractures are relatively narrowly spaced with spacing between 0.03 and 0.31 m with most data lying between 0.03 and 0.15 m and with a mean value of 0.12 m (Fig. 8). The spacing of the W–E-trending fractures was more difficult to measure in the field; data obtained, how-

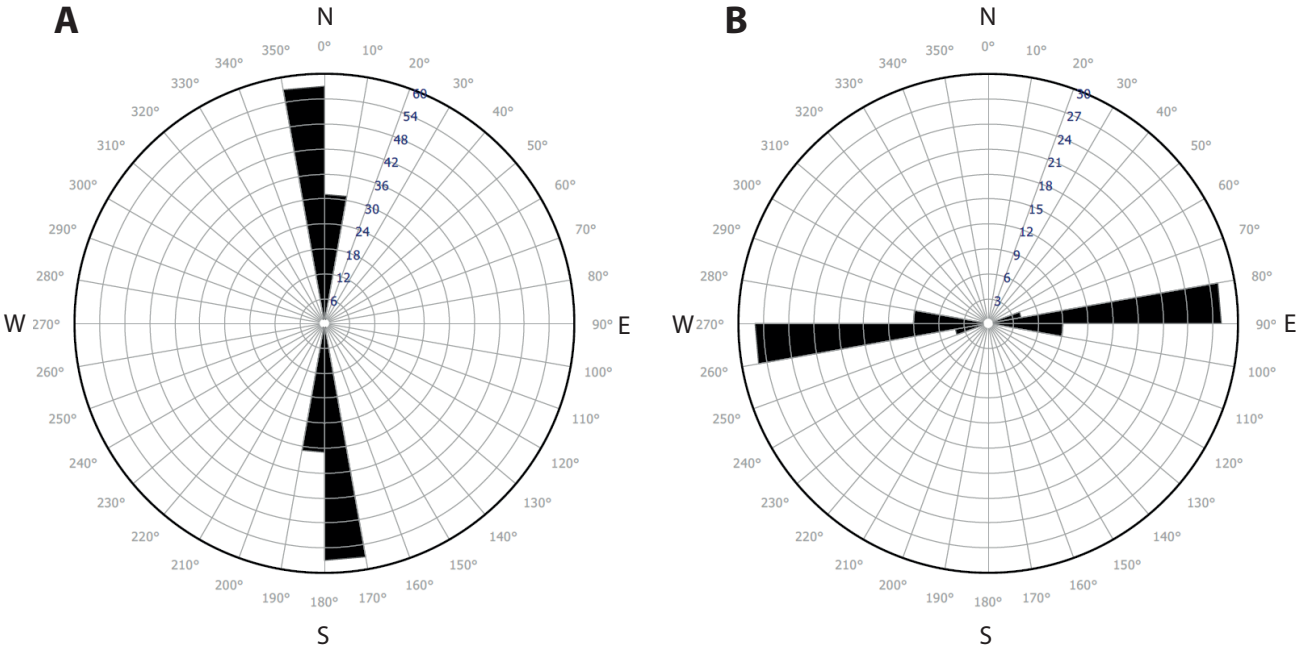

Fig. 4. Rose diagrams showing the orientation of the near-vertical to steeply dipping fractures in the Arnager Limestone Formation. **A,** One fracture set is aligned N–S (combined data from all six study sites). **B,** A second fracture set is aligned W–E (combined data from all six study sites with cliff exposures).

ever, show that most of these fractures have spacing between 0.10 and 0.30 m. Bedding plane exposures in the lowermost part of the limestone show a structure with spacing between the two fracture lines rather similar to those obtained in cliff exposures (Fig. 7).

In the lower part of the limestone, bed thickness (and thereby spacing of bedding-parallel fractures) varies between 0.06 and 0.40 m, with most beds having thicknesses between 0.06 and 0.14 m and a mean value of 0.16 m (Fig. 9).

The two sets of near-vertical to steeply dipping fractures in the Arnager Limestone terminate against the hardground in the middle of the boundary conglomerate (Fig. 7). The basal part of the boundary conglomerate as well as the underlying Arnager Greensand are characterised by a complete lack of these fracture sets.

An important observation of the outcrop is the complete absence of stylolites and polygonal fractures as well as slickenlines that would indicate shear movement. However, plume and hackle marks are observed indicating tensile stress in a zone of compression.

Mechanical properties

New data from the Arnager limestone include porosity, elastic wave velocities, elastic moduli, Poisson's ratio and dry tensile strength. No significant difference in dry tensile strength is found between the investigated orientations (Fig. 10, Table 1). Cross-plotting a calculated bulk density assuming 100% water saturation and tensile strength in the dry state shows a significantly higher tensile strength of the silica-rich Arnager Limestone compared to chalk from København Limestone Formation and from Tor Formation at Stevns (Fig. 10). Voake *et al*. (2019) investigated the difference in tensile strength between dry and water saturated Mons (Belgium) and Kansas (USA) chalk and found 1–2 MPa lower tensile strength of water saturated than dry Mons chalk with porosity similar to the tested Arnager Limestone samples. Because such effects of water saturation mainly are found in calcite-bonded rocks, no significant reduction in the dry tensile strength due to water saturation is expected in the silica bonded chalk of Arnager Limestone.

Fig. 5. Fracture system in lowermost part of the Arnager Limestone Formation. The limestone is well bedded with low-angle dipping mound structures. It has two near-vertical to steeply dipping and orthogonal fracture sets trending N–S and W–E respectively; in addition the limestone displays near-horizontal to gently dipping bedding-parallel fractures. The fractures impose a blocky appearance to the limestone. Length of scale is 50 cm. Cliff is viewed from the southwest. Picture taken at midday Sun.

Discussion

Origin of near-vertical to steeply dipping fracture sets

The near-vertical to steeply dipping fractures in the Arnager Limestone are aligned in two directions, N–S (355–175°) and W–E (265–85°) being perpendicular to each other. The fracture pattern is consistent along the cliff exposure and relatively simple. Bedding plane exposures near the base of the formation, however, display a slightly different fracture pattern with most fractures aligned NNW–SSE (325–145°) and W–E (265–85°). The dominant orientation of major Mesozoic faults bounding the Arnager-Sose block is NW–SE (315–135°); less common fault systems on this block are aligned NNW–SSE (345–165°) and W–E (275–95°; Graversen 2009). Thus, the orientation of the near-vertical to steeply dipping fractures in the Arnager Limestone is in best agreement with the orientation of the less common faults systems on the Arnager-Sose Block. The Arnager fractures also fit reasonably well with measurements of all faults limiting Mesozoic bedrock as these are aligned predominantly N–S (355–175°) and WNW–ESE (285–105°; Graversen 2009). Thus, it is suggested that the near-vertical to steeply dipping fractures are tectonic in origin, although they may have been accentuated during final unloading processes.

The near-vertical to steeply dipping fractures in the Arnager Limestone are opening-mode fractures according to the terminology of Bai & Pollard (2000) and as argued above formed in response to tectonic extension. Experimental results and field observations have shown that opening-mode fractures

Fig. 6. Two closely associated, near-vertical and through-going fractures. The fractures are trending W–E; hammer at base of the cliff for scale. Cliff is viewed from the west. Picture taken at evening Sun.

typically are confined by layer boundaries with their height equal to the height of the fractured layer and their spacing proportional to this thickness (Bai *et al.* 2000). However, in the Arnager Limestone fractures typically cross bed boundaries probably because all beds are of almost identical lithofacies (rock mechanical subunits) and bedding planes thereby only act as weak interfaces. In the Arnager Limestone the average bed thickness is about 0.16 m and the average spacing of near-vertical fractures is about 0.12 m; leading to a ratio between fracture spacing and bed thickness of about 0.8, close to the expected value for a bedded carbonate succession (cf. Bai & Pollard 2000; Cooke *et al.* 2007).

The near-vertical to steeply dipping fractures in the Arnager Limestone are gradually reduced in aperture and finally completely vanish in the upper part of the boundary conglomerate and are absent in the lowermost part of the conglomerate and in the underlying Arnager Greensand. This is explained by a change from brittle conditions in the lithified (coherent) Arnager Limestone to bulk deformation due to grain boundary sliding in the loose, unlithified (loose with no or little cohesion) Arnager Greensand.

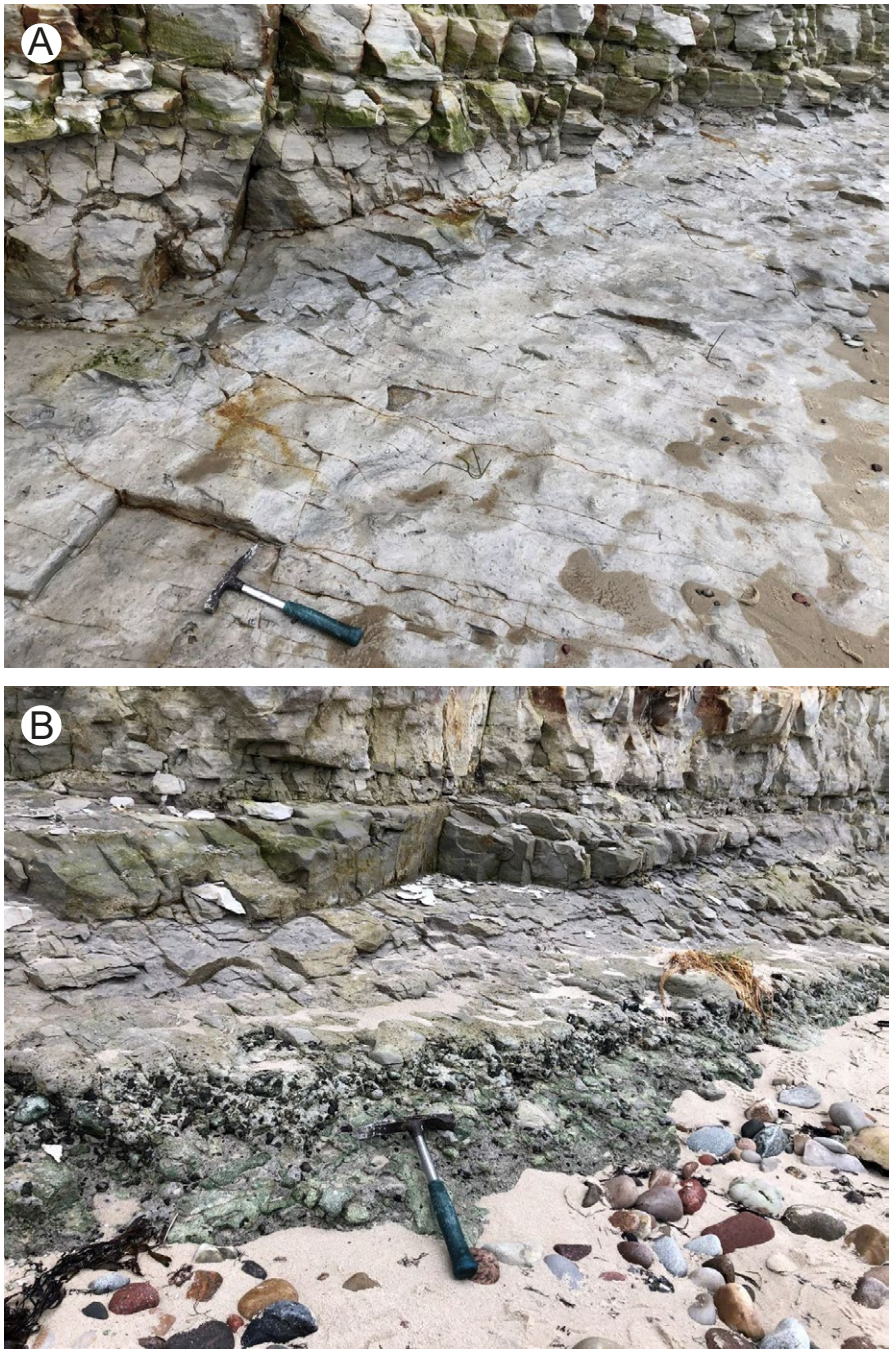

Fig. 7. A, Bedding plane exposures of the near-vertical to steeply dipping fractures in the Arnager Limestone Formation immediately above the boundary conglomerate. One fracture set is trending NNW–SSE (near parallel to hammer shaft) and a second fracture set is trending W–E. Cliff seen in upper part of the picture. Modern beach sand covers the seaward part of the exposure. Exposure is viewed from the west. **B,** The near-vertical to steeply dipping fractures in the Arnager Limestone Formation terminate at the hardground in the middle of the boundary conglomerate. One fracture set is in the Arnager Limestone Formation trending NNW–SSE, a second fracture set is trending W–E. Modern beach sediments cover the seaward part of the sedimentary rocks. Exposure is viewed from the southwest.

Origin of bedding-parallel fracture set

Bedding-parallel fractures are characteristic of the Arnager Limestone outcrop, and can be referred to as unloading fractures. That burial followed by uplift and erosion would result in horizontal fracturing may, at first glance, appear illogical, but the phenomenon is well described in the geotechnical literature (e.g. Santamarina 2003). The fractures arise because the stress geometry during burial and during uplift differ. At maximum burial depth, the vertical stress is likely the major principal stress, and the two principal horizontal stresses are the minor ones. During uplift, the vertical stress approaches zero as it would be at the surface, and the two horizontal stresses become the major principal stresses. This situation corresponds to an extension stress geometry, which would tend to result in horizontal fractures if the tensile strength is exceeded. Whether horizontal fractures form depends on the tensile strength of the rock, and with respect to this property, strain difference on the rock frame over geological time plays a role. As an illustrative case, we define the 1-direction as vertical, and 2- and 3-directions as the horizontals. Further, if we assume that the limestone is isotropic, then the relation between normal strain and normal stress of a representative element volume (REV) is given by Hoek's law as

$$\begin{bmatrix}\varepsilon_1\\ \varepsilon_2\\ \varepsilon_3\end{bmatrix} = \left(\frac{G(3M-4G)}{M-G}\right)^{-1}\begin{bmatrix}1 & -\upsilon & -\upsilon\\ -\upsilon & 1 & -\upsilon\\ -\upsilon & -\upsilon & 1\end{bmatrix}\begin{bmatrix}\sigma_1\\ \sigma_2\\ \sigma_3\end{bmatrix} \quad (5)$$

where ε_1, ε_2, ε_3 are normal strains, σ_1, σ_2, σ_3 are normal stresses, M is the compressional modulus, G is the shear modulus and ν is Poisson's ratio. Inserting $\sigma_1 = 0$

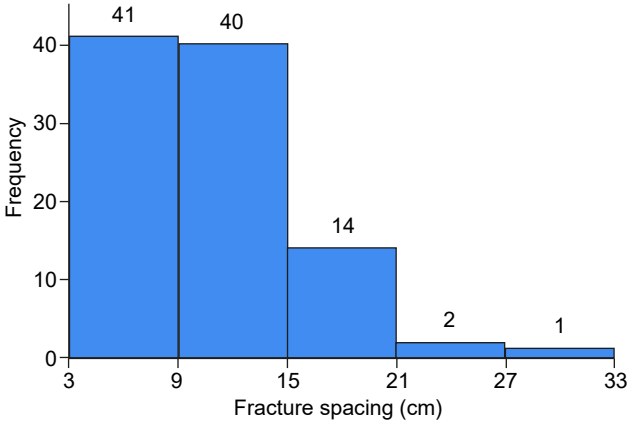

Fig. 8. Histogram showing spacing of near-vertical to steeply dipping fractures in cm. Data represent the N–S-trending fractures. Data were collected in the lowermost, mound-bedded part of the Arnager Limestone Formation.

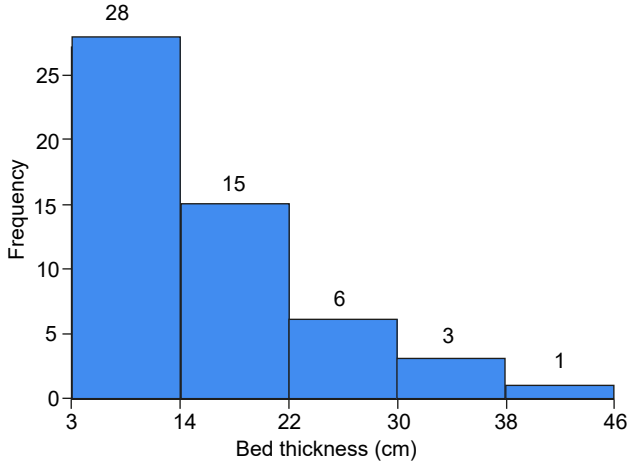

Fig. 9. Histogram of bed thickness in cm. Data were collected in the lowermost part of the Arnager Limestone Formation.

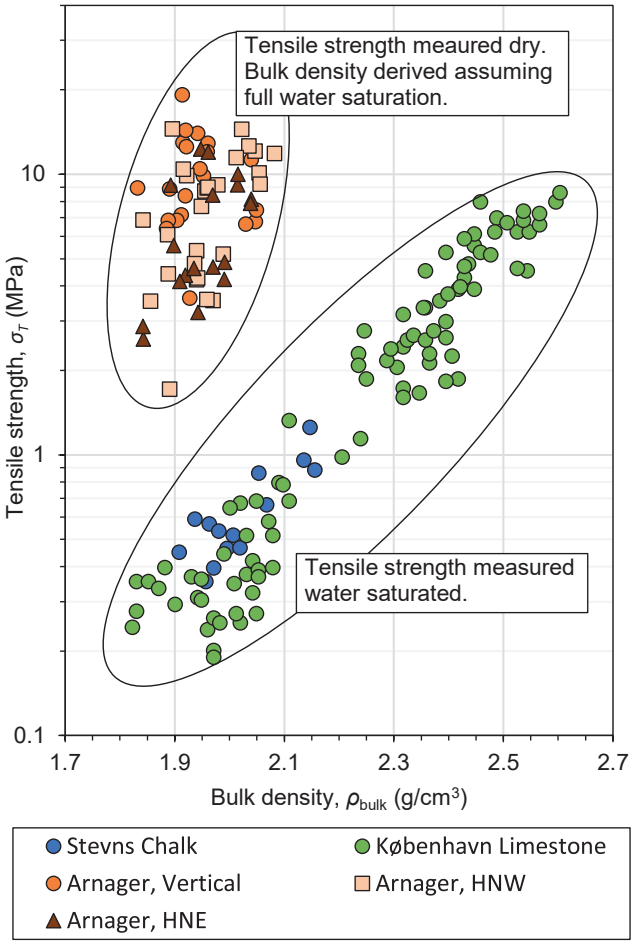

Fig. 10. Cross-plots of bulk density and tensile strength. Blue data points: Stevns chalk (Katić *et al.* 2019), green: København Limestone (Database; Courtesy of Geo). Orange data points: Arnager Limestone where HNW is horizontal north-west direction, and HNE is horizontal north-east direction.

and $\sigma_2,\sigma_3 > 0$ in equation 5, thus representing the time after uplift, we may derive the difference in strain as

$$\begin{bmatrix}\varepsilon_1\\ \varepsilon_2\\ \varepsilon_3\end{bmatrix} = \left(\frac{G(3M-4G)}{M-G}\right)^{-1}\begin{bmatrix}1 & -\upsilon & -\upsilon\\ -\upsilon & 1 & -\upsilon\\ -\upsilon & -\upsilon & 1\end{bmatrix}\begin{bmatrix}0\\ \sigma_2 > 0\\ \sigma_3 > 0\end{bmatrix} \quad (6)$$

from which we see that the vertical normal strain (ε_1) becomes negative during uplift with a magnitude of

$$\varepsilon_1 = \left(\frac{G(3M-4G)}{M-G}\right)^{-1}(-\upsilon(\sigma_2+\sigma_3))\,. \quad (7)$$

The negative vertical strain is caused by the compressive horizontal stresses (σ_2, σ_3), and by assuming that the limestone behaves linear elastic until failure, the negative normal strain may exceed the tensile strength, resulting in horizontal fractures.

The rock may also have reduced tensional strength from a mechanism related to strain difference between particles and cement during uplift. Neglecting temperature increase from burial, the mechanism is that sedimentary particles (in this case, siliceous carbonate ooze) during burial (load increase) are subjected to elastic strain (ε_{fr}), then at a critical strain (ε_{crit}), contact cementation (bonding) takes place, and during subsequent burial, both particles and cement are strained (ε_{fr} and ε_C). The interesting point is that the accumulated strain of the particles is higher than that of the cement. Upon stress relief due to uplift and erosion, the particles relax, causing the cement to endure tensile strain, consequently promoting horizontal fracturing (Fig. 11). This process will likely form micro-cracks from which fractures due to negative (tensional) normal strain may initiate.

It has been argued that bedding-parallel fractures also could be a result from glacial deformation since former glacial deposits directly overlie the Arnager Limestone at the outcrop. If glacial deformation (shearing) was the cause for formation of the bedding-parallel fractures it would have been expected that slicken sides would be present, but these have not been observed. The Arnager Limestone has been subject to unloading due to erosion of overlying deposits and repeated loading/unloading cycles during glaciations since Bornholm was covered by the Scandinavian Ice Sheet during the Quaternary glaciations (Houmark Nielsen & Kjær 2003). The removal of sediments covering the Arnager Limestone (e.g. the Bavnodde Greensand) would create favourable conditions for generating the bedding-parallel fractures described above. A speculative increased fluid overpressure beneath the ice would also favour the formation of fractures, including the bedding-parallel due to the reduction in stress caused by excess pore pressure. However, as horizontal (flat-lying) fractures would, in any case, be expected to form due to the uplift, it is hardly necessary to invoke this extra mechanism.

Comparative studies

Fracture patterns in non-siliceous Upper Cretaceous, Tor Formation chalk deposits exposed at Sigerslev quarry (Stevns), Denmark (Fig. 1) have some similarities to the fracture pattern in the Arnager Limestone. At the Sigerslev quarry, the system consists of closely spaced horizontal fractures and four sets of vertical

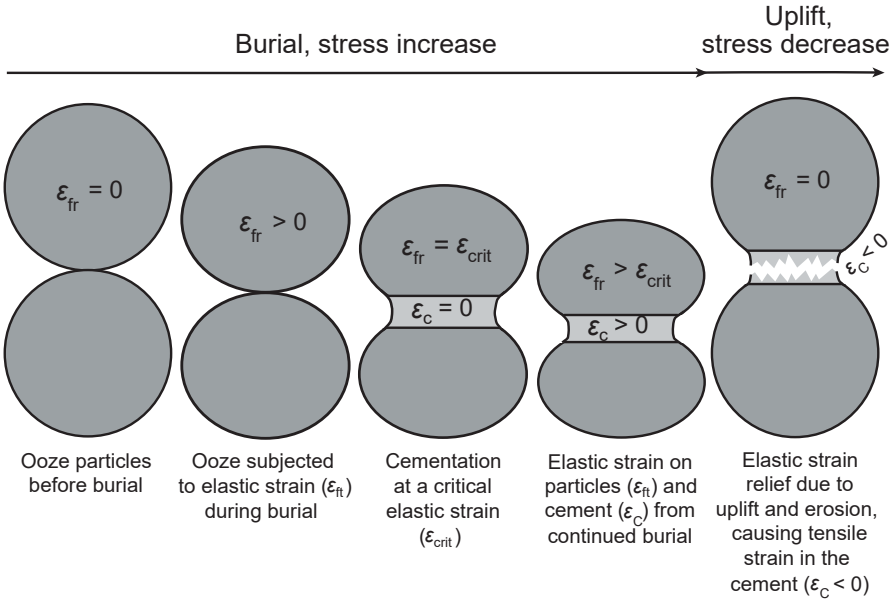

Fig. 11. Conceptual illustration of uniaxial strain development during burial and subsequent uplift on a sedimentary rock frame. Temperature increase from burial is neglected. Positive and negative strain represent compaction and tension, respectively. ε_{fr} is the particle/rock frame strain, and ε_C is the cement strain forming at a critical strain ε_{crit}. Tensile ruptures/fractures are created by tensile strain in the cement ($\varepsilon_C < 0$) due to uplift/ stress decrease and the difference in strain between ε_{fr} and ε_C.

fractures (Rosenbom & Jacobsen 2005). The vertical to steeply dipping fractures are striking 25, 60, 145 and 175°. Unfortunately, no information on fracture spacing is reported, but own observations in the uppermost part of the chalk at Stevns Klint show typical spacings of the steeply dipping fractures rather similar to those observed in the Arnager Limestone. The formation of the vertical fractures at the Sigerslev quarry was related to regional dextral transpressionel stresses along major north-south oriented faults causing partial inversion of the area, while the horizontal fractures would have formed by removal of 500–750 m of overlying sediments by uplift and erosion (Rosenbom & Jacobsen 2005).

The København Limestone Formation (Late Danian) is a partly indurated limestone that has been studied in excavations on Amager (Jakobsen & Klitten 1999; Fig.1); the limestone displays horizontal fractures as well as vertical fractures. The horizontal fractures are typically situated at the boundary between strongly indurated and slightly indurated beds formed during relaxation due to unloading of overlying sediments; loading and unloading of ice during the Quaternary may also have contributed to their formation (Jakobsen & Klitten 1999). The vertical fractures formed in connection with tectonic movements in the Fennoscandian Border (Tornquist) Zone (Jacobsen & Klitten 1999).

Thus, in both the København Limestone and the chalk at Sigerslev two sets of fractures are present: horizontal fractures classified as unloading fractures and vertical to steeply dipping fractures classified as tectonic. In a similar way, the fracture system in the Arnager Limestone is composite. An early tectonic phase created the near-vertical to steeply dipping fracture sets, while the bedding-parallel fractures in the Arnager Limestone most likely formed during a period when the least compressive stress was vertical as they are open fractures that break along bedding planes. Thus, their origin is interpreted to be related to the erosion of overlying sediments. A final phase was most likely tectonic tilting of the complete succession resulting in the present day low-angle dip of 5° towards the NW.

Palaeoburial

The rock mechanical data (table 1), i.e. the tensile strength, elastic moduli and Poisson's ratio, provide the basis for discussing the maximal burial depth of Arnager Limestone. However, a minimum palaeoburial of the Arnager Limestone is constrained by the 180 m thickness of the Bavnodde Greensand (Christensen 1985), whereas a maximum palaeoburial constraint of the Arnager Limestone of 1000 m may be envis-

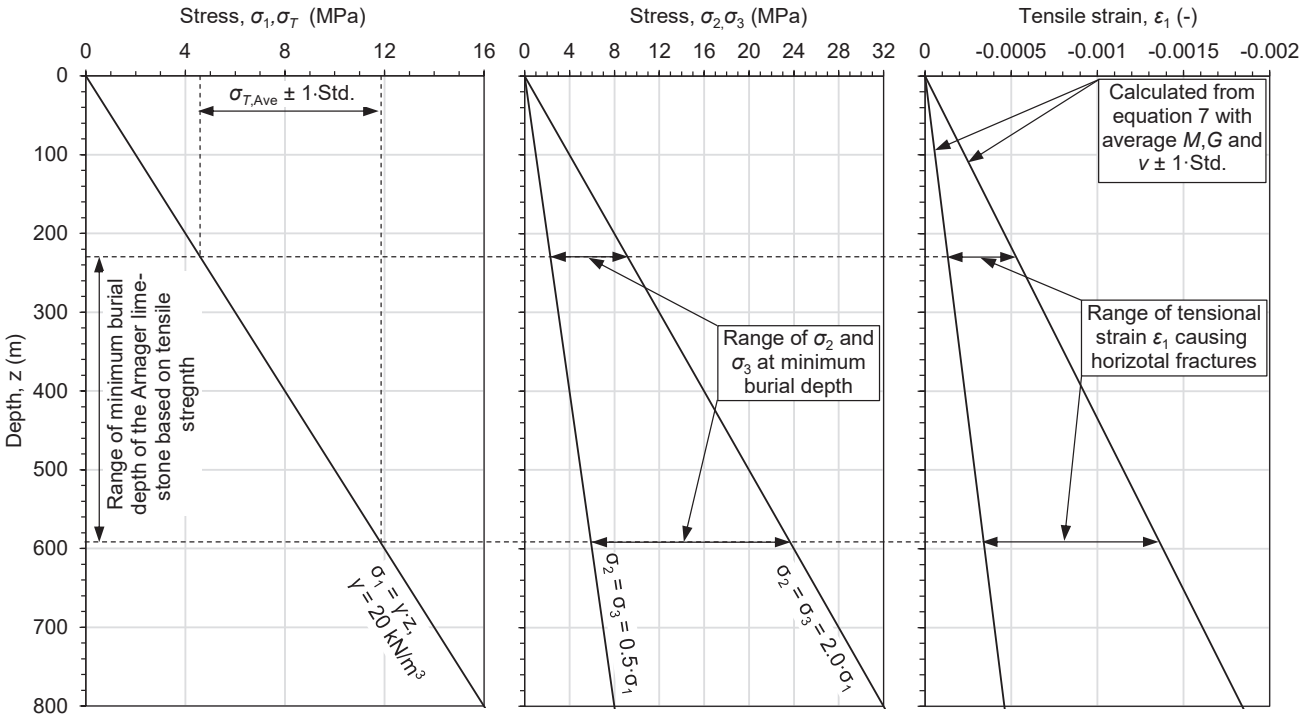

Fig. 12. Stress and strain plots versus depth plots. Left: vertical stress and tensile strength showing the estimated minimum Arnager Limestone burial depth. Middle: horizontal stresses derived from a K0 of 0.5 and 2. Right: vertical tensional strain that is required to generate horizontal fractures from uplift.

aged by the transition from opal-CT to quartz, which requires thermal energy provided by heating through time. In deep chalks of the Ontong Java Plateau the transition is found at 1100 m below sea floor in Eocene sediments, where the present temperature is less than 30˚C (Kroenke *et al*. 1991; Fabricius & Borre 2007). Suppose we assume a higher sea floor temperature on the Coniacian shelf of Bornholm area and take the much longer time into account; even with a low geothermal gradient, burial can hardly have exceeded a maximum of 1000 m, as also indicated by the absence of stylolites in the Arnager Limestone and lack of cementation of Lower Cretaceous and Jurassic sands on Bornholm.

By assuming a linear vertical stress increase with depth from an average unit weight (γ) of 2.0 kN/m^3, the minimum range of palaeoburial of the Arnager Limestone may be estimated from the range of measured tensile strength (Fig. 12). Observations have identified bedding-parallel horizontal fractures (Fig. 2) in the Arnager cliff, meaning that the tensile strength has been exceeded through geological history. Following equation 6 and combining the range of measured tensile strength with estimated vertical stress from burial, the palaeoburial depth is estimated to be approximately 230 to 600 m (Fig. 12). This estimated palaeoburial is thus within the constraints given by the Bavnodde Greensand thickness and the transition from opal-CT to quartz. A guess on the ratio of horizontal to vertical stress (K0) of 0.5 to 2 and assuming equal horizontal stresses ($\sigma_2 = \sigma_3$) illustrates that the vertical tensional strain (ε_1) that is required to generate horizontal fractures from uplift ($\sigma_1 = 0$, $\sigma_2 = \sigma_3 < 0$) and calculated from equation 7 ranges from $4.1{\cdot}10^{-5}$ to $1.4{\cdot}10^{-3}$.

Conclusions

- Exposures of naturally fractured carbonate sedimentary rocks function as analogues for subsurface carbonate reservoirs and can yield insights about the fracture characteristics, patterns, dimensions and cross-cutting relationships and thereby aid interpretations of past tectonic events and burial history.

- The Arnager Limestone shows a system of natural fractures including two near-vertical to steeply dipping orthogonal fracture sets as well as a bedding-parallel, flat-lying to gently dipping fracture set.

- The Arnager Limestone forms a 12–20 m thick, main rock mechanical unit subdivided into near-identical, cm- to dm-thick, mechanical subunits separated by bed boundaries that act as weak interfaces.

- Most of the near-vertical to steeply dipping fractures are confined to 2–5 beds; some span the complete outcrop (main mechanical unit). This pattern underlines the relative constant mechanical properties of the Arnager Limestone, and the weak nature of the interfaces along bedding planes.

- The near-vertical to steeply dipping fracture sets are oriented north–south and west–east respectively. The observed fracture pattern agrees with the overall Mesozoic block fault pattern on Bornholm supporting a tectonic origin of the vertical fracture sets. This type of fractures is not present in the underlying Arnager Greensand as this unit forms a ductile mechanical unit.

- The flat-lying to gently dipping fractures developed along bed boundaries and formed as a result of unloading due to uplift and erosion of covering sediments, possibly accentuated by glacial processes.

- Based on rock mechanical laboratory data and comparative studies, the palaeoburial for the Arnager Limestone is estimated to be 230–600 m.

Acknowledgements

The authors would like to thank Peter Frykman and an anonymous reviewer for their constructive reviews of the manuscript. Ole Bennike and Henrik Tirsgaard are thanked for handling the editorial process. The authors are very grateful to Michael John Welch and Emil Mejlhede Kinslev (DTU) for constructive input to the manuscript and valuable discussions on natural fractures in chalk. Catherine Chagué is thanked for constructive comments on an early version of the manuscript. Joakim Korshøj (GEO) is thanked for assisting with preparation of core plug samples.

References

Aguilera, R. 1998: Geologic aspects of naturally fractured reservoirs. The Leading Edge 17(12), 1667–1670. https://doi.org/10.1190/1.1437912

Babuska, V. & Plomerova, J. 2004: The Sorgenfrei–Tornquist Zone as the mantle edge of Baltica lithosphere: new evidence from three-dimensional seismic anisotropy. Terra Nova 16, 243–249. https://doi.org/10.1111/j.1365-3121.2004.00558.x

Bai, T. & Pollard, D.D. 2000: Fracture spacing in layered rocks: a new explanation based on the stress transition. Journal of Structural Geology 22, 43–57. https://doi.org/10.1016/S0191-8141(99)00137-6

Bourbiaux, B. 2010: Fractured Reservoir Simulation: a Challenging and Rewarding Issue. Oil & Gas Science and Technology – Rev. IFP 65, 227–238. https://doi.org/10.2516/ogst/2009063

Bromley, R.G. 1979: Field meeting in southern Scandinavia 18–28 September 1975. Proceedings of the Geologists' Association 90, 181–191. https://doi.org/10.1016/S0016-7878(79)80004-8

Chaika, C. & Dvorkin, J. 1997: Ultrasonic velocities of opaline rocks undergoing silica diagenesis. Geophysical Research Letters 24, 2039–2042. https://doi.org/10.1029/97GL01959

Christensen, W.K. 1985: The Albian to Maastrichtian of southern Sweden and Bornholm, Denmark; a review. Cretaceous Research 5, 313–327. https://doi.org/10.1016/S0195-6671(84)80027-0

Cooke, M.L., Simo, J.A., Underwood, C.A. & Rijken, S. 2006: Mechanical stratigraphical control on fracture patterns within carbonates and implications for groundwater flow. Sedimentary Geology 184, 325–339. https://doi.org/10.1016/j.sedgeo.2005.11.004

Cotte, N., Pedersen, H.A. & the TOR Working Group 2002: Sharp contrast in lithospheric structure across the Sorgenfrei–Tornquist Zone as inferred by Rayleight wave analysis of TOR1 project data. Tectonophysics 360, 75–88. https://doi.org/10.1016/S0040-1951(02)00348-7

Dean, J.R. 1998: Extraction methods for environmental analysis, 225 pp. Chichester: Wiley.

Erlström, M., Thomas, S.A., Deeks, N. & Sivhed, U. 1997: Structure and tectonic evolution of the Tornquist Zone and adjacent sedimentary basins in Scania and the southern Baltic Sea area. Tectonophysics 271, 191–215. https://doi.org/10.1016/S0040-1951(96)00247-8

Fabricius, I.L. & Borre, M.K. 2007: Stylolites, porosity, depositional texture, and silicates in chalk facies sediments. Ontong Java Plateau – Gorm and Tyra fields, North Sea. Sedimentology 54, 183–205. https://doi.org/10.1111/j.1365-3091.2006.00828.x

Gabrielsen, R.H. & Koestler, A.G. 1987: Description and structural implications for fractures in late Jurassic sandstones of the Troll Field, northern North Sea. Norsk Geologisk Tidsskrift 67, 371–381.

Glad, A.C., Amour, F., Welch, M.J., Clausen, O. R., Anderskouv, K., Ineson, J. R., Sheldon, E. & Nick, H.M. 2022: Natural fractures in a Lower Cretaceous chalk-marlstone reservoir, Valdemar Field, Danish North Sea. Marine and Petroleum Geology 136, 105445. https://doi.org/10.1016/j.marpetgeo.2021.105445

Graversen, O. 2009: Structural analysis of superposed fault systems of the Bornholm horst block, Tornquist Zone, Denmark. Bulletin of the Geological Society of Denmark 57, 25–49. https://doi.org/10.37570/bgsd-2009-57-02

Graversen, O. 2004: Upper Triassic – Lower Cretaceous seismic sequence stratigraphy and basin tectonics at Bornholm, Denmark, Tornquist Zone, NW Europe. Marine and Petroleum Geology 21, 579–612. https://doi.org/10.1016/j.marpetgeo.2003.12.001

Hart, M.B., Bromley, R.G. & Packer, S.R. 2012: Anatomy of the stratigraphical boundary between the Arnager Greensand and Arnager Limestone (Upper Cretaceous) on Bornholm, Denmark. Proceedings of the Geologists Association 123, 471–478. https://doi.org/10.1016/j.pgeola.2011.11.006

Houmark-Nielsen, M. 2011: Pleistocene glaciations in Denmark: a closer look at chronology, ice dynamics and landforms. In: Ehlers, J., Gibbard, P.L. & Hughes, P.D. (eds): Quaternary glaciations – extent and chronology – a closer look. Developments in Quaternary Sciences 15, 47–58. https://doi.org/10.1016/B978-0-444-53447-7.00005-2

Houmark-Nielsen, M. & Kjær, K.H. 2003: Southwest Scandinavia, 40–15 kyr BP: palaeogeography and environmental change. Journal of Quaternary Science 18, 769–786. https://doi.org/10.1002/jqs.802

Humlum, O. & Houmark-Nielsen, M. 1994: High deglaciation rates in Denmark during the Late Weichselian – implications for the palaeoenvironment. Geografisk Tidsskrift 94, 26–37. https://doi.org/10.1080/00167223.1994.10649349

ISRM Commission on Testing Methods 1978: Suggested methods for determining tensile strength of rock materials. International Journal of Rock Mechanics and Mining Sciences & Geomechanics 15, 99–103. http://dx.doi.org/10.1016/0148-9062(78)90003-7

Jakobsen P.R. & Klitten, K. 1999: Fracture systems and groundwater flow in the København Limestone Formation. Nordic Hydrology 30, 301–316. https://doi.org/10.2166/nh.1999.0017

Jensen, J.B. & Hamann, N.E. 1989: Geological mapping of Mesozoic deposits along the eastern margin of the Rønne Graben, offshore Bornholm, Denmark. Bulletin of the Geological Society of Denmark 37, 237–260. https://doi.org/10.37570/bgsd-1988-37-19

Katić, N., Korshøj, J.S., Christensen, H.F. 2019: Bryozoan limestone experience – the case
of Stevns Klint. AIMS Geosciences 5,163–183. https://doi.org/10.3934/geosci.2019.2.163

Kroenke, L.W. *et al.* 1991: Proceedings of the Ocean Drilling Program, Initial Reports 130, 1240 pp. College Station, Texas. https://doi.org/10.2973/odp.proc.ir.130.1991

Lemonnier, P. & Bourbiaux, B. 2010: Simulation of naturally fractured reservoirs. state of the art – part 2 – matrix-fracture transfers and typical features of numerical studies. Oil & Gas Science and Technology – Rev. IFP 65, 263–286. https://doi.org/10.2516/ogst/2009067

Lykke-Andersen, H. & Surlyk, F. 2004: The Cretaceous–Palaeogene boundary at Stevns Klint, Denmark: inversion tectonics or sea-floor topography? Journal of the Geological Society of London 161, 343–352. https://doi.org/10.1144/0016-764903-021

Madsen, H.B., Stemmerik, L. & Surlyk, F. 2010: Diagenesis of silica-rich mound-bedded chalk, the Coniacian Arnager limestone, Denmark. Sedimentary Geology 223, 51–60. https://doi.org/10.1016/j.sedgeo.2009.10.002

Mavko, G., Mukerji, T. & Dvorkin, J. 2009: The rock physics handbook: Tools for seismic analysis of porous media, 329

pp. Cambridge University Press. https://doi.org/10.1017/CBO9780511626753

Noe-Nygaard, N. & Surlyk, F. 1985: Mound bedding in a sponge rich Coniacian chalk, Bornholm, Denmark. Bulletin of the Geological Society of Denmark 34, 237–249. https://doi.org/10.37570/bgsd-1985-34-19

Ogata, K., Senger, K., Braathen, A., Tveranger, J. & Olaussen, S. 2014: The importance of natural fractures in a tight reservoir for potential CO_2 storage: a case study of the upper Triassic-middle Jurassic Kapp Toscana Group (Spitsbergen, Arctic Norway). In: Spence, G.H. *et al.* (eds): Advances in the study of fractured reservoirs. Geological Society of London, Special Publications 374, 395–415. https://doi.org/10.1144/SP374.9

Packer, S.R. & Hart, M.B., 2005: Coniacian–Santonian Radiolaria from the Upper Cretaceous of Bornholm, Denmark. A preliminary investigation. Bulletin of the Geological Survey of Denmark 52, 141–157. https://doi.org/10.37570/bgsd-2005-52-11

Peacock, D.C.P., Nixon, C.W., Rotevatn, A., Sanderson, D.J. & Zuluaga, L.F. 2016: Glossary of fault and other fracture networks. Journal of Structural Geology 92, 12–29. https://doi.org/10.1016/j.jsg.2016.09.008

Rosenbom, A.E. & Jacobsen, P.R. 2005: IR thermography and fracture analysis of preferential flow in chalk. Vadose Zone Journal 4, 271– 280. https://doi.org/10.2136/vzj2004.0074

Santamarina, J.C. 2003: Soil behavior at the microscale: particle forces. In: Germaine, J.T., Sheahan, T.C. & Whitman, R.V. (eds): Proceedings of the Symposium on Soil Behavior and Soft Ground Construction, in honor of Charles C. Ladd - October 2001. American Society of Civil Engineers Special Publication 119, 25–56. https://doi.org/10.1061/40659(2003)2

Solymar, M. & Fabricius, I.L. 1999: Image analysis and estimation of porosity and permeability of Arnager Greensand, Upper Cretaceous, Denmark. Physics and Chemistry of the Earth Part A – solid Earth and Geodesy 24, 587–591. https://doi.org/10.1016/S1464-1895(99)00084-8

Svennevig, K. & Surlyk, F. 2018: A high-stress shelly fauna associated with sponge mud-mounds in the Coniacian Arnager Limestone of Bornholm, Denmark. Lethaia 52, 57–76. https://doi.org/10.1111/let.12290

Tröger, K.A. & Christensen, W.K. 1991: Upper Cretaceous (Cenomanian Santonian) inoceramid bivalve faunas from the island of Bornholm, Denmark. Danmarks Geologiske Undersøgelse A28, 47 pp. https://doi.org/10.34194/seriea.v28.7048

Vejbæk, O.V. 1985: Seismic stratigraphy and tectonics of sedimentary basins around Bornholm, southern Baltic. Danmarks Geologiske Undersøgelse A8, 30 pp. https://doi.org/10.34194/seriea.v8.7027

Voake, T., Nermoen, A., Ravnås, C., Korsnes, R.I. & Fabricius, I.L. 2019: Influence of temperature cycling and pore fluid on tensile strength of chalk. Journal of Rock Mechanics and Geotechnical Engineering, 11, 277–288. https://doi.org/10.1016/j.jrmge.2018.12.004

Waight, T.E., Serre, S.H., Naesby, S.H. & Thomsen, T.B. 2017: The ongoing search for the oldest rock on the Danish island of Bornholm: new U-Pb zircon ages for a quartz-rich xenolith and country rock from the Svaneke Granite. Bulletin of the Geological Society of Denmark 65, 75–86. https://doi.org/10.37570/bgsd-2017-65-06

Welch, M.J., Souque, C., Davies, R.K. & Knibe, R.J. 2015: Using mechanical models to investigate the controls on fracture geometry and distribution in chalk. In: Agar, S.M & Geiger, S. (eds): Fundamental controls on fluid flow in carbonates: current workflows to emerging technologies. Geological Society of London, Special Publications 406, 281–309. https://doi.org/10.1144/SP406.5

Ziegler, P.A. 1990: Geological atlas of western and central Europe, 2nd edition, 239 pp. The Hague: Shell International Petroleum Maatschappij B.V.